Supporting Information

Aluminium Acetylacetonate Ligands Passivation for $CsPbBr_3$ Nanocrystals with Improved Stability and Photoluminescence

Hao Yu[1], Bin Yan[1], Yonghui Song[3], Qiqi Zhao[2], Meng Gao[1], Liangmin Ning[1], Wei Chen[1], Min Fu[1], Kunhua Wang[1,*], and Jianxu Ding[2,*]

[1]College of Energy Storage Technology, Shandong University of Science and Technology, Qingdao 266590, China

[2]College of Materials Science and Engineering, Shandong University of Science and Technology, Qingdao 266590, China

[3]Department of Applied Chemistry, Hefei Science Center of Chinese Academy of Sciences, University of Science and Technology of China, Hefei, Anhui 230026, China

[4] Key Laboratory of Materials Physics of Ministry of Education, School of Physics and Microelectronics, Zhengzhou University, Daxue Road 75, Zhengzhou 450052, China.

*Corresponding authors:

wangkhua@mail.ustc.edu.cn (Kunhua Wang)

dingjianxu@sdust.edu.cn (Jianxu Ding)

Materials and Chemicals: oleic acid (OA, analytically pure (AR), Aladdin), oleylamine (OAm, 80%-90%, Aladdin), 1-octadecene (ODE, 90%, Aladdin), cesium carbonate (Cs_2CO_3, 99.9%, Aladdin), isopropyl alcohol (C_3H_8O, 99.7%, KESHI), n-hexane (C_7H_8, 97%, KESHI), toluene (C_7H_8, 99.5%, KESHI), 2-bromoacetophenone (98%, Aladdin), aluminium triacetylacetone ($Al(acac)_3$, 98%, Aladdin), lead acetate trihydrate ($Pb(CH_3COO)_2{\cdot}3H_2O$, 99.99%, Aladdin), n-octane (C_8H_{18}, Sinopharm Chemical Reagent Co., Ltd), acetone (99.5%, KESHI). PEDOT:PSS solutions (Al4083 CLEVIOS), PTAA (Xi'an Polymer Light Technology Corp), lithium fluoride (LiF, Luminescence Technology Corp.), 4,6-bis(3,5-di(pyridin-3-yl)phenyl)-2-methylpyrimidine (B3PymPm, Luminescence Technology Corp.). All reagents were used as received without further purification.

LED Fabrication and Performance Test: Firstly, the indium tin oxide (ITO) patterned glasses were ultrasonic washed three times by deionized water, isopropyl alcohol and acetone, respectively. Afterwards, the substrate was dried under N_2 and addressed by UV-ozone for 15 min. PEDOT:PSS was spin-coated onto the surface of ITO substrates at 4000 rpm for 50 s and heated at 140 °C for 20 min under ambient conditions. PTAA was dissolved in chlorobenzene (6 mg mL^{-1}), instantly, the mixture above was spun onto the layer of PEDOT:PSS by spin-coater at 2000 rpm for 60 s and annealed at 120 °C for 20 min under N_2. For constituting a perovskite NC emission layer, $CsPbBr_3$ NCs in octane (10 mg mL^{-1}) were spin-coated onto the PTAA layer at 1000 rpm for 60 s and baked at 60 °C for 5 min. Ultimately, under a high vacuum (~2×10^{-4} Pa), PO-T2T (40 nm) and LiF/Al electrodes (1 nm/100 nm) were deposited using a thermal evaporation system with a shadow mask. The active area of as-prepared device was 4 mm^2. The working efficiency of as-prepared LED device was explored on Keithley 2400 Source Meter for the purpose of obtaining the current versus voltage characteristics. The luminescence characteristics of the device (the light flux of the silicon photodiode and the electroluminescence (EL) spectrum of the device) were obtained using a PR-670 spectroscopic sweep luminance meter and a Marine optical Jaz spectrometer, severally. Under the assumption that the emission of the LED

presents a Lambert pattern, according to L-J-V and EL measurements, EQE used to characterize LED can be calculated. External quantum efficiency (η_{EQE}) is the ratio of the number of photons emitted from the LEDs to the number of charge carriers injected into the device, and it can be expressed as:

$$\eta_{EQE} = \frac{q}{hcf} \cdot \frac{\int \lambda S(\lambda) d\lambda}{\int S(\lambda) R(\lambda) d\lambda} \cdot \frac{I_{det}}{J_D A} \quad (1)$$

where q is the electric charge, h is Planck's constant, c is the speed of light, f is the geometry factor (representing the fraction of emitted photons reaching the detector), I_{det} is the photocurrent, A is the device area, and J_D is the injection current density to LEDs. η_{EQE} can also be calculated from the luminous power efficiency, which is

$$\eta_{EQE} = \frac{qV}{hc} \cdot \frac{\int \lambda S(\lambda) d\lambda}{\int G(\lambda) S(\lambda) d\lambda} \cdot \eta_{PE} \quad (2)$$

Power efficiency (η_{PE}) is defined as the ratio of the output luminous flux to the input power of LEDs. can be expressed as:

$$\eta_{PE} = \frac{L}{J_D} \cdot \frac{\pi}{V} \quad (3)$$

where V is the applied voltage to LEDs, L is luminance.

Characterizations.

The transmission electron microscope (TEM) was measured using Thermo fisher talos F200X G2 with an accelerating voltage of 120 kV. High resolution electron microscopy (HRTEM), mapping mode energy dispersive X-ray spectroscopy (EDS) and large angle circular dark field scanning electron microscopy (HAADF-STEM) were characterized on TALOS F200X transmission electron microscopy at 120 kV. X-ray diffraction (XRD) pattern analysis was performed on a Miniflex 600 operating at Cu Kα radiation (λ=1.54178 Å). The scanning electron microscopy (SEM) was observed on a Apreo S HiVac at an acceleration voltage of 5 kV. X-ray photoelectron spectroscopy (XPS) of $CsPbBr_3$ NCs deposited on silicon wafers was conducted with Thermo ESCALAB250 at a monochrome Al-KR radiation source (1486.7 eV). Ultraviolet absorption spectra (UV−vis) was demonstrated on PekinElmer by collecting $CsPbBr_3$ NCs dispersed in n-hexane in a transmission mode. The PL spectra and PLQYs

were carried out on a Hamamatsu(C11347) absolute PLQY spectrometer by photoexcitation of octane suspension in a quartz colorimetric dish at a wavelength of 365 nm. Using Nicolet iS50 FT-IR with KBr pellet acquired the FTIR spectra. ^{1}H nuclear magnetic resonance (^{1}H NMR) was detected by JNM-ECZ400S. 5 mg of $CsPbBr_3$ NCs powder was dissolved in deuterium chloroform ($CDCl_3$) for sample preparation.

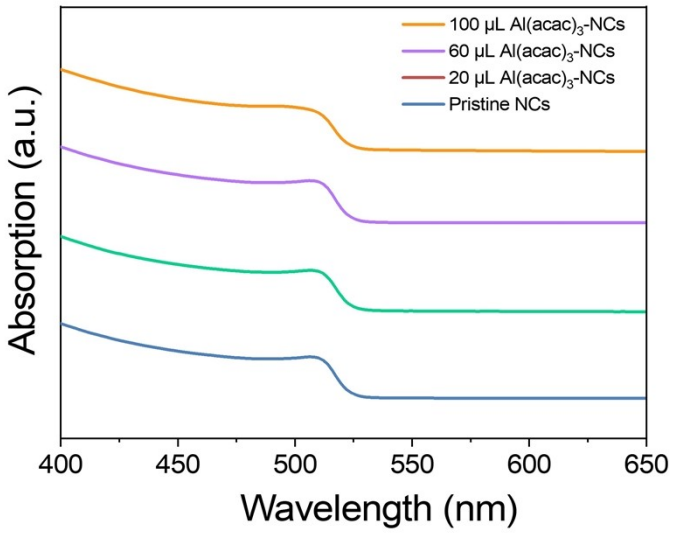

Figure S1. Normalized UV-vis absorption spectra of pristine and $Al(acac)_3$-NCs with different amount of $Al(acac)_3$ in toluene.

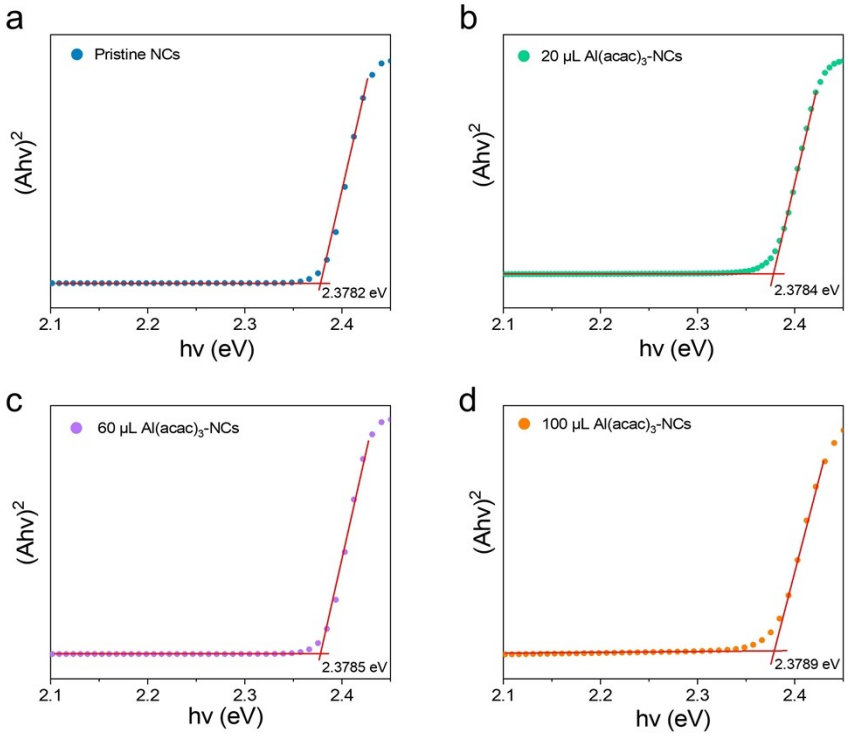

Figure S2. The band gap of pristine NCs and $Al(acac)_3$-NCs with different amount of $Al(acac)_3$ in toluene.

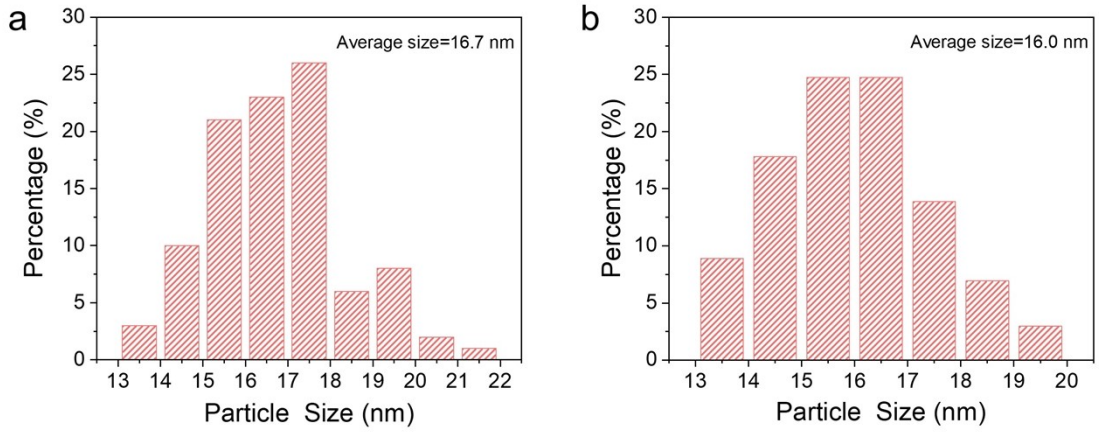

Figure S3. Particle size distribution histograms of the (a) pristine NCs and (b) $Al(acac)_3$-NCs.

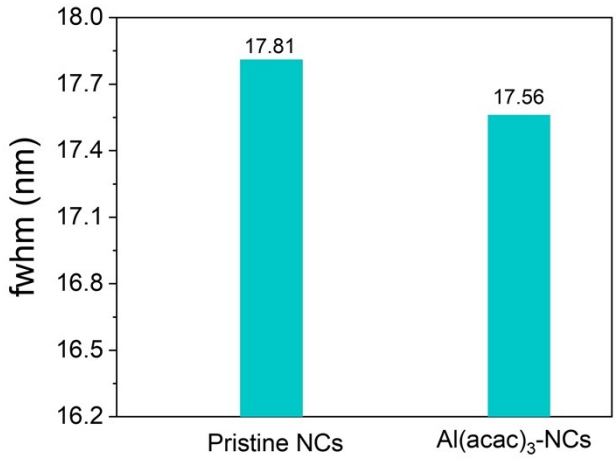

Figure S4. Full width at half-maximum (fwhm) of pristine NCs and $Al(acac)_3$-NCs.

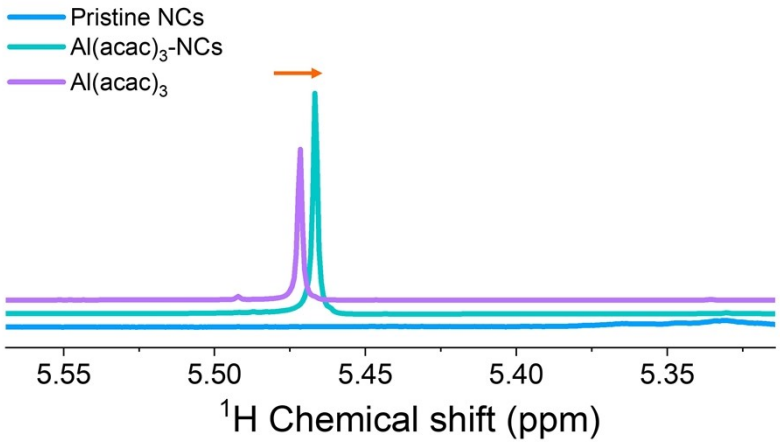

Figure S5. Magnified ^1H liquid-state NMR spectra of $Al(acac)_3$ ligand, pristine, and $Al(acac)_3$-NCs.

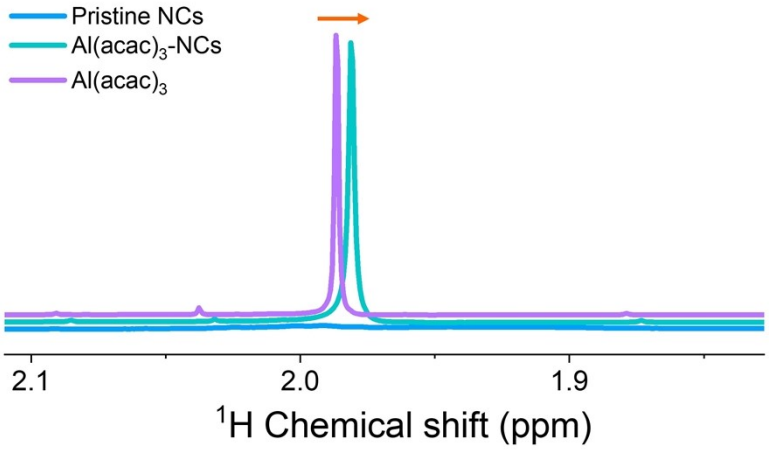

Figure S6. Magnified ^{1}H liquid-state NMR spectra of $Al(acac)_3$ ligand, pristine, and $Al(acac)_3$-NCs.

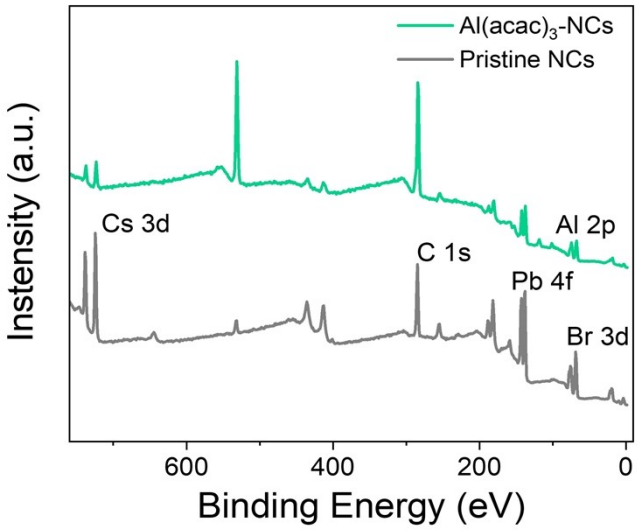

Figure S7. Survey XPS spectra of pristine and $Al(acac)_3$-NCs.

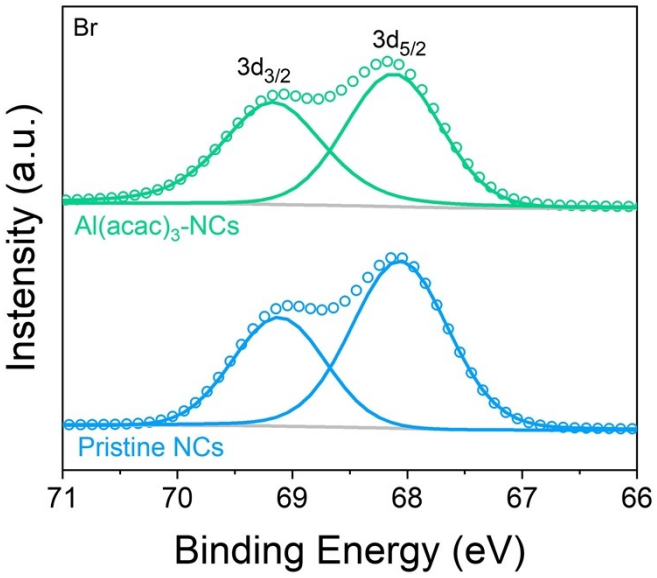

Figure S8. The high-resolution XPS spectra of Br 3d of pristine and $Al(acac)_3$-NCs.

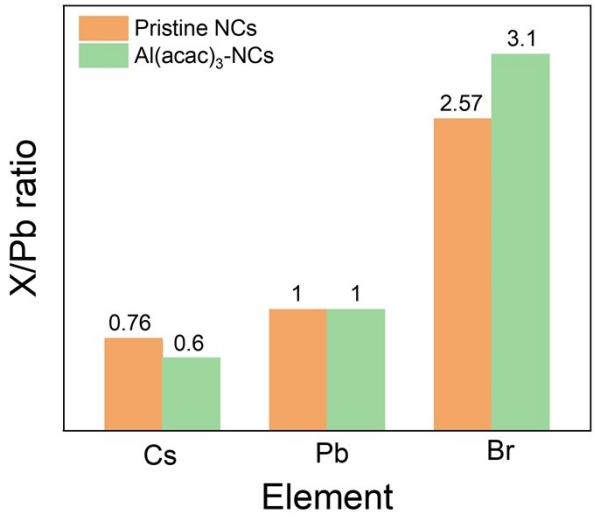

Figure S9. The atomic ratio of X/Pb measured by XPS for pristine and $Al(acac)_3$-NCs.

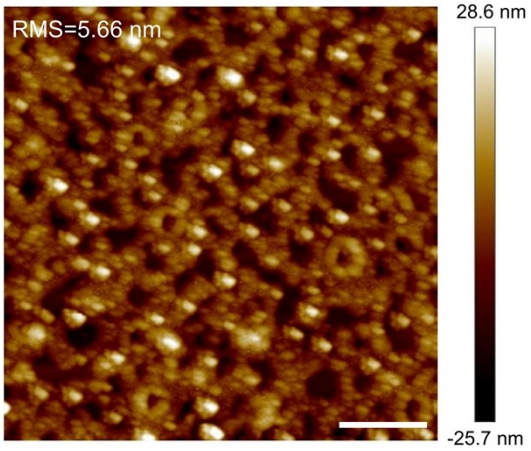

Figure S10. AFM image of $Al(acac)_3$-NC film. The scale bar represents 1 μm.

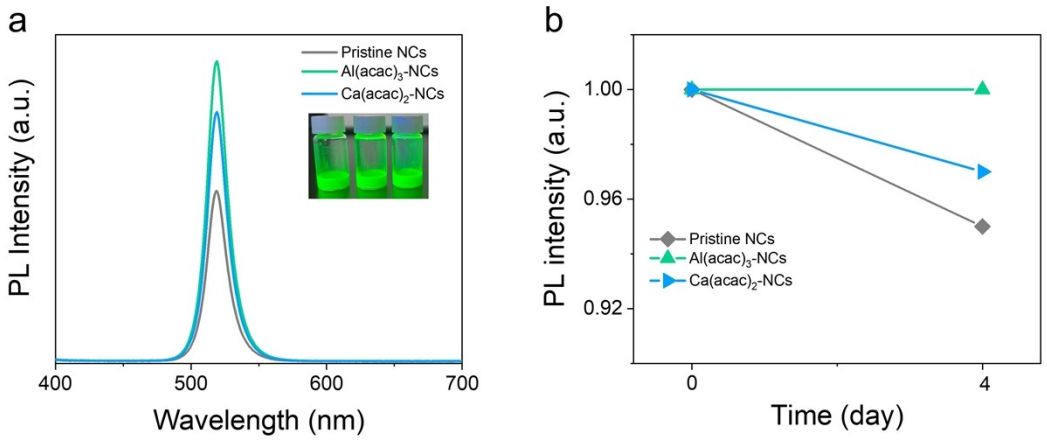

Figure S11. (a) PL intensity of $CsPbBr_3$ NCs and NCs treated by $Al(acac)_3$ as well as $Ca(acac)_2$. Inset: From left to right, the pictures of pristine NCs, $Al(acac)_3$-NCs, and $Ca(acac)_2$-NCs. (b) Relative PL changes with time for $CsPbBr_3$ NCs treated by $Al(acac)_3$ and $Ca(acac)_2$.

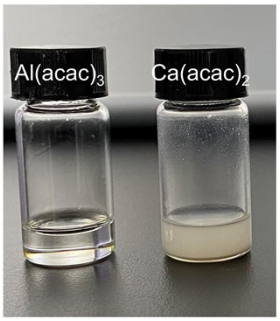

Figure S12. Photograph of $Al(acac)_3$ and $Ca(acac)_2$ dissolved in toluene. $Al(acac)_3$ ligand can dissolve well in toluene and $Ca(acac)_2$ ligand cannot be completely dissolved.

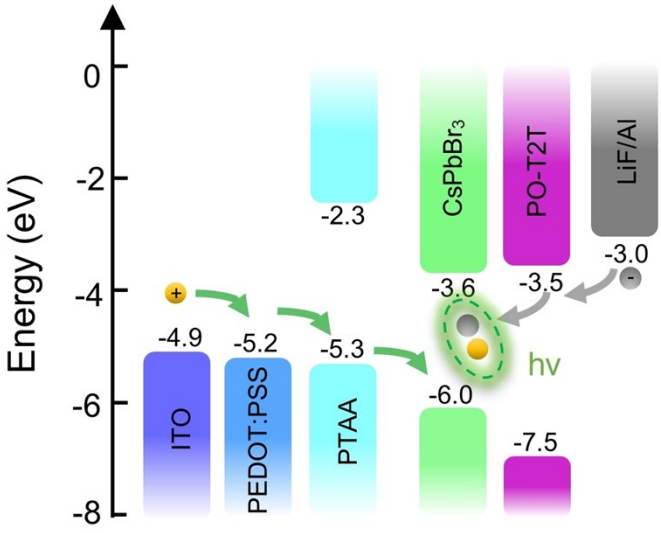

Figure S13. Energy-level diagram of the LED device structure.

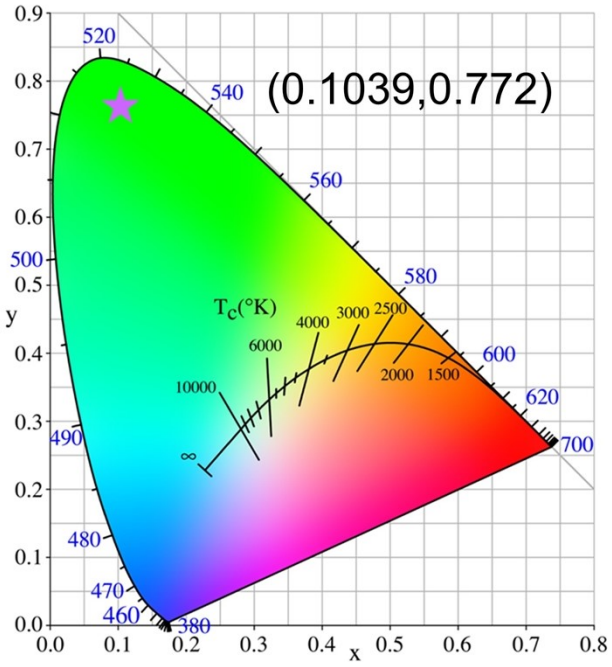

Figure S14. The corresponding Commission Internationale de l'Eclairage (CIE) coordinate of the fabricated LEDs by $Al(acac)_3$-NC films.

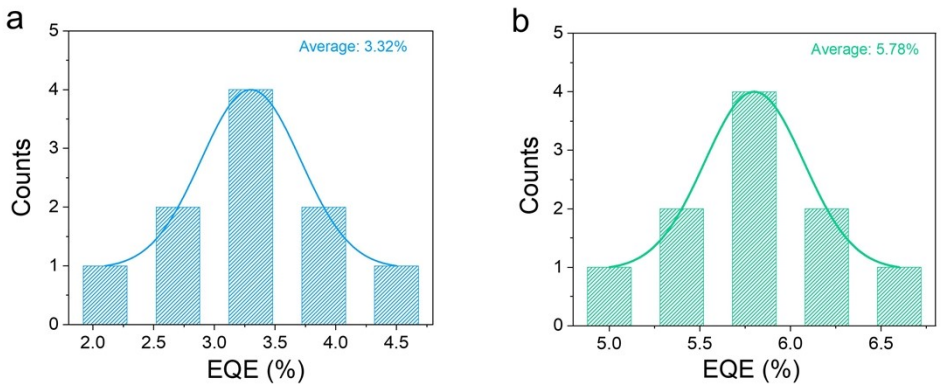

Figure S15. Histogram of maximum EQEs of LED based on (a) pristine NC films and (b) $Al(acac)_3$-NC films.

Supplementary Tables

Table S1. PLQY summary of green perovskite NC and films.

Material	PLQY of NCs (%)	PLQY of NC films (%)	PLQY of films (%)	Reference
$CsPbBr_3$ NCs	**93.5**	**88**	-	**This work**
$CsPbBr_3$ NCs	85	68	-	1
$CsPbBr_3$ NCs	95	48	-	2
$CsPbBr_3$ QDs	100	52	-	3
$CsPbBr_3$ NCs	83	95	-	4
$MAPbBr_3$ NCs	90	48	-	5
$CsPbBr_3$ QDs	80	52	-	6
$CsPbBr_3$ NCs	75	65	-	7
$CsPbBr_3/CsPb_2Br_5$ NCs	54	39	-	8
FA/ $CsPbBr_3$ QDs	90	61	-	9
$CsPbBr_3$ QDs	-	85.2	-	10
$PEA_2(CsPbBr_3)_{n-1}PbBr_4$ film	-	-	-	11
$CsPbBr_3$/ETPTA film	-	-	90.02	12
$CsPbBr_3$ film	-	-	54	13
$CsPbBr_3$ film	-	-	73.6	14
$CsPbBr_3$ film	-	-	30	15
$(BA)_2(MA)_3(Pb)_4(Br)_{13}$ film	-	-	60.9	16

Table S2. The fitting of the PL decay lifetime for pristine $CsPbBr_3$ and $Al(acac)_3$-$CsPbBr_3$ NC films.[a]

Sample	τ_1	τ_2	τ_{ave}
Pristine NC	13.20±0.46 (81%)	86.43±1.57 (19%)	26.82±1.63
$Al(acac)_3$-NC	16.16±0.61 (86%)	122.45±3.12 (14%)	30.59±3.18

[a] The PL was excited at 405 nm and monitored at the maximum emission peak. The average PL lifetimes (τ_{avg}) were obtained by $\tau_{avg} = (A_1 \times \tau_1^{\,2} + A_2 \times \tau_2^{\,2})/(A_1 \times \tau_1 + A_2 \times \tau_2)$, where A_1 and A_2 stand for the statistical weights of the corresponding lifetime components (given in the parentheses).

Table S3. Performance summary of recently reported green perovskite NC LEDs.

Perovskite Material	Device structure	Device performance Parameters			Ref.
		EL (nm)	FWHM (nm)	Turn-on Voltage (V)	
$CsPbBr_3$ NCs	**ITO/PEDOT:PSS/PTAA/LiF/ $CsPbBr_3$ NCs/B3PymPm/LiF/Al**	**517**	**16.8**	**＜2.0**	**Our work**
$CsPbBr_3$ NCs	ITO/PEDOT:PSS/PTAA/LiF/ $CsPbBr_3$PNCs/B3PymPm/LiF/Al	521	16.4	2.4	1
$CsPbBr_3$ QDs	FTO/SnO_2/QDs/ZnO/Ag	520	21	2.8	3
FA/$CsPbBr_3$ QDs	ITO/PEDOT:PSS/PTAA/QDs /TBPi/LiF/Al	515	18	-	9
$CsPbBr_3$ NCs	ITO/m-PEDOT:PSS/Perovskite /ETPTA/LiF/ Al	508	20	-	12
$CsPbBr_3$ NCs	ITO/HTL/Perovskite/TPBi/LiF/Al	513	18	2.3	13
$CsPbBr_3$ QDs	ITO/PEDOT:PSS/PTAA/ $CsPbBr_3$PNCs/TPBi/LiF/Al	~504	20	2.4	17
$CsPbBr_3$ NCs	ITO/PEDOT:PSS/PTAA/ $CsPbBr_3$ PNCs/TPBi/LiF/Al	518	~18	-	18
$FAPbBr_3$ NCs	ITO/PEDOT:PSS/poly-TPD/TBB/ Perovskite/TPBi/LiF/Al	531	~21	2.6	19

References:

1. Yang, J. N.; Chen, T.; Ge, J.; Wang, J. J.; Yin, Y. C.; Lan, Y. F.; Ru, X. C.; Ma, Z. Y.; Zhang, Q.; Yao, H. B., High Color Purity and Efficient Green Light-Emitting Diode Using Perovskite Nanocrystals with the Size Overly Exceeding Bohr Exciton Diameter. *Journal of the American Chemical Society* **2021,** *143* (47), 19928-19937.
2. Yao, J. S.; Zhang, J. C.; Wang, L.; Wang, K. H.; Ru, X. C.; Yang, J. N.; Wang, J. J.; Chen, X.; Song, Y. H.; Yin, Y. C.; Lan, Y. F.; Zhang, Q.; Yao, H. B., Suppressing Auger Recombination in Cesium Lead Bromide Perovskite Nanocrystal Film for Bright Light-Emitting Diodes. *Journal of Physical Chemistry Letters* **2020,** *11* (21), 9371-9378.
3. Zheng, C.; Bi, C. H.; Huang, F.; Binks, D.; Tian, J. J., Stable and Strong Emission $CsPbBr_3$ Quantum Dots by Surface Engineering for High-Performance Optoelectronic Films. *Acs Applied Materials & Interfaces* **2019,** *11* (28), 25410-25416.
4. Di Stasio, F.; Christodoulou, S.; Huo, N.; Konstantatos, G., Near-Unity Photoluminescence Quantum Yield in $CsPbBr_3$ Nanocrystal Solid-State Films via Postsynthesis Treatment with Lead Bromide. *Chemistry of Materials* **2017,** *29* (18), 7663-7667.
5. Tezuka, Y.; Umemoto, K.; Takeda, M.; Takahashi, Y.; Ebe, H.; Enomoto, J.; Rodbuntum, S.; Nohara, T.; Fontecha, D.; Asakura, S.; Chiba, T.; Furis, M. I.; Yoshida, T.; Uji-i, H.; Masuhara, A., Effects of alkylamine chain length on perovskite nanocrystals after washing and perovskite light-emitting diodes. *Japanese Journal of Applied Physics* **2020,** *59* (SD).
6. Shi, S.; Wang, Y.; Zeng, S.; Cui, Y.; Xiao, Y., Surface Regulation of $CsPbBr_3$ Quantum Dots for Standard Blue-Emission with Boosted PLQY. Advanced Optical Materials 2020, 8 (12), 2000167.
7. Enomoto, K.; Oizumi, R.; Aizawa, N.; Chiba, T.; Pu, Y.-J., Energy Transfer from Blue-Emitting $CsPbBr_3$ Perovskite Nanocrystals to Green-Emitting $CsPbBr_3$ Perovskite Nanocrystals. *The Journal of Physical Chemistry C* **2021,** *125* (35), 19368-19373.
8. Jiang, G.; Guhrenz, C.; Kirch, A.; Sonntag, L.; Bauer, C.; Fan, X.; Wang, J.; Reineke, S.; Gaponik, N.; Eychmüller, A., Highly Luminescent and Water-Resistant $CsPbBr_3$–$CsPb_2Br_5$ Perovskite Nanocrystals Coordinated with Partially Hydrolyzed Poly(methyl methacrylate) and Polyethylenimine. *ACS Nano* **2019,** *13* (9), 10386-10396.
9. Song, J.; Li, J.; Xu, L.; Li, J.; Zhang, F.; Han, B.; Shan, Q.; Zeng, H., Room-Temperature Triple-Ligand Surface Engineering Synergistically Boosts Ink Stability, Recombination Dynamics, and Charge Injection toward EQE-11.6% Perovskite QLEDs. *Adv Mater* **2018,** *30* (30), e1800764.
10. Zeng, Q.; Luo, X.; Du, Y.; Jiang, J.; Yang, L.; Zhao, H.; Shi, H.; Li, Y., Ionic liquid-induced in situ deposition of perovskite quantum dot films with a photoluminescence quantum yield of over 85. *Nanoscale* **2021,** *13* (47), 20067-20077.
11. Yang, X.; Zhang, X.; Deng, J.; Chu, Z.; Jiang, Q.; Meng, J.; Wang, P.; Zhang, L.; Yin, Z.; You, J., Efficient green light-emitting diodes based on quasi-two-dimensional composition and phase engineered perovskite with surface passivation. *Nat Commun*

2018, *9* (1), 570.
12. Chu, Z.; Ye, Q.; Zhao, Y.; Ma, F.; Yin, Z.; Zhang, X.; You, J., Perovskite Light-Emitting Diodes with External Quantum Efficiency Exceeding 22% via Small-Molecule Passivation. *Adv Mater* **2021,** *33* (18), e2007169.
13. Han, B.; Yuan, S.; Fang, T.; Zhang, F.; Shi, Z.; Song, J., Novel Lewis Base Cyclam Self-Passivation of Perovskites without an Anti-Solvent Process for Efficient Light-Emitting Diodes. *ACS Appl Mater Interfaces* **2020,** *12* (12), 14224-14232.
14. Cai, L.; Yang, F.; Xu, Y.; Fan, J.; Li, Y.; Zhao, Y.; Liang, D.; Zou, Y.; Li, P.; Wang, L.; Wang, C.; Li, Y.; Fan, J.; Sun, B., Dual Functionalization of Electron Transport Layer via Tailoring Molecular Structure for High-Performance Perovskite Light-Emitting Diodes. *ACS Appl Mater Interfaces* **2020,** *12* (33), 37346-37353.
15. Wu, T.; Li, J.; Zou, Y.; Xu, H.; Wen, K.; Wan, S.; Bai, S.; Song, T.; McLeod, J. A.; Duhm, S.; Gao, F.; Sun, B., High-Performance Perovskite Light-Emitting Diode with Enhanced Operational Stability Using Lithium Halide Passivation. *Angew Chem Int Ed Engl* **2020,** *59* (10), 4099-4105.
16. Yukta; Chini, M. K.; Ranjan, R.; Satapathi, S., Lewis Base Passivation of Quasi-2D Ruddlesden–Popper Perovskite for Order of Magnitude Photoluminescence Enhancement and Improved Stability. *ACS Applied Electronic Materials* **2021,** *3* (4), 1572-1582.
17. Dong, Y.; Wang, Y. K.; Yuan, F.; Johnston, A.; Liu, Y.; Ma, D.; Choi, M. J.; Chen, B.; Chekini, M.; Baek, S. W.; Sagar, L. K.; Fan, J.; Hou, Y.; Wu, M.; Lee, S.; Sun, B.; Hoogland, S.; Quintero-Bermudez, R.; Ebe, H.; Todorovic, P.; Dinic, F.; Li, P.; Kung, H. T.; Saidaminov, M. I.; Kumacheva, E.; Spiecker, E.; Liao, L. S.; Voznyy, O.; Lu, Z. H.; Sargent, E. H., Bipolar-shell resurfacing for blue LEDs based on strongly confined perovskite quantum dots. *Nat Nanotechnol* **2020,** *15* (8), 668-674.
18. Song, J.; Fang, T.; Li, J.; Xu, L.; Zhang, F.; Han, B.; Shan, Q.; Zeng, H., Organic-Inorganic Hybrid Passivation Enables Perovskite QLEDs with an EQE of 16.48. *Adv Mater* **2018,** *30* (50), e1805409.
19. Wang, H.; Gong, X.; Zhao, D.; Zhao, Y.-B.; Wang, S.; Zhang, J.; Kong, L.; Wei, B.; Quintero-Bermudez, R.; Voznyy, O.; Shang, Y.; Ning, Z.; Yan, Y.; Sargent, E. H.; Yang, X., A Multi-functional Molecular Modifier Enabling Efficient Large-Area Perovskite Light-Emitting Diodes. *Joule* **2020,** *4* (9), 1977-1987.